Sonochemical Synthesis of Molybdenum Oxide− and Molybdenum Carbide−Silica Nanocomposites

N. Arul Dhas and A. Gedanken*

Department of Chemistry, Bar-Ilan University, Ramat-Gan, 52900, Israel

Received June 24, 1997. Revised Manuscript Received September 16, 1997[⊗]

A novel sonochemical approach for the preparation of molybdenum oxide ($Mo_2O_5 \cdot xH_2O$) and molybdenum carbide (Mo_2C) clusters coated on silica carriers, in which $Mo(CO)_6$ precursor serves as an in situ source for the coating phase of both materials (molybdenum oxide and molybdenum carbide), has been described. Ultrasonic irradiation of a slurry of molybdenum hexacarbonyl, $Mo(CO)_6$, and silica microspheres in decane for 3 h, under ambient air and argon, yields diphasic molybdenum oxide−silica (MOS) and molybdenum carbide−silica (MCS) composites, respectively. Characterization using powder X-ray diffraction and transmission electron microscopy, with selected area electron diffraction, shows the amorphous nature of the nanocomposites. The phase evolution by long-term thermal reduction of MOS under H_2 shows that the Mo_2O_5 undergoes stepwise reduction following the sequence, $Mo^V \rightarrow Mo^{IV} \rightarrow Mo^o$. The TEM image of MOS and MCS shows that the sonochemical decomposition products of $Mo(CO)_6$ attached on the silica carrier as clusters, as thin layers, or as nanoparticles depends upon the precursor composition. UV−visible absorption studies on the sonochemically produced MOS demonstrate that the characteristic absorption of the Mo^V (d^1 cation) oxide system and the Mo ions are likely to possess two types of coordination symmetry (T_d and O_h). Considerable changes in the characteristic UV−visible absorption of MOS, compared to that of bulk molybdenum oxide and bare silica, was observed, perhaps associated with the chemical interaction, to form a desirable interfacial bond. FT-IR spectroscopy illustrated the structural changes that occur when the amorphous SiO_2 is coated sonochemically. It has been proposed that the coating takes place via ultrasonic-cavitation-induced decomposition of the precursor into the required coating phase and the breaking of the strained siloxane link of the silica; subsequently, the coating phase and silica particles collide with each other and deposit themselves into the coating.

Introduction

Coated ceramic materials are receiving increased attention because of their importance for both a fundamental understanding of their properties and for their applications.[1] Because of the composition gradient imposed by coating, the surfaces of these materials may possess completely different characteristics than does the core element. This can be exploited to synthesize materials with unique optical, electronic, magnetic, catalytic, and mechanical properties. Although the technology for coating rather large substrates is well-established, especially in the microelectronic industry,[2] coating of very small substrates, such as submicron particles, still remains a technical challenge. During the last few decades, a great deal of fundamental and applied research interest was focused on supported-molybdenum oxide catalyst because of its numerous applications in petroleum refining, chemical production, and pollution control industries.[3] Molybdenum carbide has also received special attention as a potential substitute for noble metals, especially Ru, as a catalyst material.[4] To have an optimum catalytic performance, certain "design criteria" must be fulfilled by the catalyst material.[5] They are (i) retention of the nanoscale dimension of the active phase, since the smaller the size of the catalytic active species, the larger the fraction of the atoms exposed at surfaces, where they are accessible to reactant molecules and available for catalysis; (ii) effective interaction between the active phase and the solid support; and (iii) uniform distribution of the active phase on the surface of the support. One may reasonably expect different catalytic properties, depending on the dispersion state and the interaction of the active phase and the support.

With these perspectives, many researchers have been interested in using preparation methods that are able to ensure good dispersion of molybdenum catalyst. Different procedures may be used for depositing active compounds on a support.[6−11] The molybdenum oxide

* e-mail: gedanken@ashur.cc.biu.ac.il. FAX: +972-3-5351250.

[⊗] Abstract published in *Advance ACS Abstracts,* November 15, 1997.

(1) Chediak, J. A. *Ceram. Bull.* **1996**, *75*, 52.

(2) Koldas, T. T.; Hampden-Smith, M., *The Chemistry of Metal CVD*; VCH: Weinheim, 1994.

(3) Ng, K. Y. S.; Gulari, E. *J. Catal.* **1985**, *92*, 340. Zhang, B.; Li, Y.; Lin, Q.; Jin, D. *J. Mol. Catal.* **1988**, *46*, 229. Anpo, M.; Kondo, M.; Kubokawa, Y.; Louis, C.; Che, M. *J. Chem. Soc., Faraday Trans. 1* **1988**, *84*, 2771.

(4) Lee, J. S.; Lee, K. H.; Lee, J. Y. *J. Phys. Chem.* **1992**, *96*, 362. (and references therein).

(5) Gates, B. C. *Chem. Rev. (Washington, D.C.)* **1995**, *95*, 511. Che, M.; Louis, C. *J. Phys. Chem.* **1987**, *91*, 2875.

(6) Liu, T.; Forissier, M. Coudurier, G.; Vedrine, J. C. *J. Chem. Soc., Faraday Trans. 1* **1989**, *85*, 1607. Reddy, B. M.; Narasima, K.; Rao, P. K. *Langmuir* **1991**, *7*, 1551. Leyer, J.; Zaki, M. I.; Knozinger, H. *J. Phys. Chem.* **1986**, *90*, 4775.

(7) Brunelle, J. P. *Pure Appl. Chem.* **1978**, *50*, 1211.

(8) (a) Arena, F.; Parmaliana, *J. Phys. Chem.* **1996**, *100*, 19994. (b) Spevack, P. A.; McIntyre, N. S. *J. Phys. Chem.* **1992**, *96*, 9029.

(9) Yermakov, Yu. I. *Catal. Rev. Sci. Eng.* **1987**, *13*, 77.

(10) Louis, C.; Che, M.; Verduraz, F. B. *J. Chem. Phys.* **1982**, *79*, 803.

S0897-4756(97)00448-1 CCC: $14.00

catalyst is frequently adsorbed on a high surface area ceramic support, usually silica, alumina, etc., by wet impregnation techniques and further thermal treatments to generate the required Mo species during use or prior to use as a working catalyst.[6−8] The more classical method consists of impregnating the support with an aqueous solution of ammonium heptamolybdate at a given pH and then annealing the solid in air to get rid of the ammonia. Particular attention has to be paid to the isoelectric point of the support which influences the primary interaction of the support surface with the ionic precursor deposited compound, as emphasized by Brunelle.[7] Other preparation procedures have consisted of having organometallic complexes of Mo, such as Mo(π-C_3H_5)$_4$, reacting with a support.[9] For instance, $MoCl_5$ in gaseous phase or dissolved in cyclohexane was contacted with hydrated silica, resulting in a chemical reaction with silanol groups and well-dispersed Mo ions on the support.[10] An alternative to the conventional preparation of supported-molybdenum oxides involves recent work on thin-film specimens.[11] This utilizes ion-beam deposition of the precursors onto an appropriate substrate of alumina or graphite, followed by calcination to obtain the catalyst.

Preparation of supported molybdenum carbide involves the carbothermal reduction of supported molybdenum oxide, which is more difficult because a moderately strong chemical interaction between the molybdenum oxide and usual support material, such as silica or alumina, dictates an extremely high reduction temperature.[12] To avoid this problem, Nakamura et al.[13] employed $Mo(CO)_6$ as a catalyst precursor, which was deposited onto a dehyroxylated alumina and then decomposed in H_2 at 1220 K to yield metallic molybdenum clusters. Lee et al.[12b] carburized this Mo−Al_2O_3 with CH_4/H_2 to obtain Mo_2C−Al_2O_3. McHenry and coworkers[14] have prepared Mo_2C clusters and other refractory carbides using a modified Huffman−Kratschmer carbon arc process.

Recently, sonochemical processing has been proven to be a useful technique to generate novel materials with unusual properties.[15] The chemical effects of ultrasound arise from acoustic cavitation, that is, the formation, growth, and implosive collapse of bubbles in liquid. The implosive collapse of the bubble generates localized hot spots through adiabatic compression or shock wave formation within the gas phase of the collapsing bubble. The conditions formed in these hot spots have been experimentally determined, with transient temperatures of ~5000 K, pressures of 1800 atm, and cooling rates in excess of 10^{10} K/s. These extreme conditions attained during bubble collapse have been exploited to decompose the metal−carbonyl bonds and generate metals,[15b,c] metal carbides,[15d] and metal oxides.[15e,f] Although sonochemical techniques have been used to generate monolithic materials, sonochemical synthesis of coated ceramic composites have not been studied.

Table 1. Precursor Composition and Sonochemical Reaction Conditions Employed for the Sonochemical Coatings of Silica

sample code	amount of silica (mg)	amount of $Mo(CO)_6$ (mg)	sonication time (h)	bulk temp ±5 (°C)
C1	300	1000	3	90
C2	300	800	3	90
C3	300	500	2	90
C4	300	300	2	90

Ultrasound irradiation of molybdenum hexacarbonyl under an argon atmosphere yielded molybdenum carbide Mo_2C.[15d] In a recent study[15f] we have reported the sonochemical preparation of pentavalent molybdenum oxide (blue oxide) by irradiation of molybdenum hexacarbonyl under ambient air and its ability to generate silica-supported blue oxide. The formation of water-stabilized pentavalent molybdenum oxide, $Mo_2O_5 \cdot 2H_2O$, was confirmed by TG-DSC, XPS, potentiometric titration, UV−visible, and electron spin resonance (EPR) spectroscopy studies.[15f] Therefore, one can generate different Mo species by changing the atmosphere of the sonochemical reaction of $Mo(CO)_6$. Herein, we report on sonochemical coatings of the nanoparticles of molybdenum oxide (Mo_2O_5) and molybdenum carbide (Mo_2C) on silica microspheres by the ultrasound irradiation of slurry of $Mo(CO)_6$ and silica spheres in decane at near room temperature. Also, our interest has been focused on the effect of thermal reduction patterns, coating properties of Mo_2O_5 and Mo_2C, the effect of $Mo(CO)_6$ concentration on coating characteristics, and the spectroscopic features of sonochemically produced molybdenum oxide−silica (MOS) and molybdenum carbide−silica (MCS) nanocomposites. Characterization was accomplished using various different techniques, such as powder X-ray diffraction (XRD), transmission electron microscopy (TEM), UV−visible, and infrared (FT-IR) spectroscopy.

Experimental Section

Materials. Dried and degassed decane (98%, Sigma) was used for the sonication. Ultrasonic irradiation was accomplished with a high-intensity ultrasonic probe (Misonix, XL sonifier, 1 cm diameter Ti horn, 20 kHz, 100 W cm^{-2}). A round-bottomed Pyrex glass vessel (total volume 110 mL) was used for the ultrasound irradiation, which was carried out under ambient air and an argon atmosphere. The precursor composition and the experimental parameters are summarized in Table 1. Unless otherwise mentioned, the precursor concentration of MOS and MCS samples correspond to C1 composition. Stober's silica[16] was prepared by base hydrolysis and condensation of tetraethyl orthosilicate (TEOS) in an aqueous ethanol medium containing ammonia. The as-made Stober's silica was heated at 750 °C for 6 h in ambient air to remove the surface-bonded water. The resulting amorphous preheated silica is termed "activated silica," which is free from the population of surface hydroxyl groups.

Sonochemical Synthesis of MOS. Ultrasonic irradiation of $Mo(CO)_6$ and activated silica in decane medium yields Mo_2O_5-coated silica composite. Typically, a slurry of molyb-

(11) Spevack, P. A.; McIntyre, N. S. *J. Phys. Chem.* **1993**, *97*, 11020.
(12) (a) Lee, J. S.; Yeom, M. H.; Park, K. Y.; Nam, I. S.; Chung, J. S.; Kim, Y. G.; Moon, S. H. *J. Catal.* **1991**, *128*, 126. (b) Lee, J. S.; Yoem, M. H.; Lee, D. S. *J. Mol. Catal.* **1990**, *62*, L45.
(13) Nakamura, R.; Bowmann, R. G.; Burwell, Jr. R. I. *J. Am. Chem. Soc.* **1981**, *103*, 673.
(14) See for example, Derrington, S.; MeHenry, M. E.; Scott, J. H.; Majetich, S. A. In *Fullerenes: Physics, Chemistry, and New Direction*; Ruoff, R. S., Kadish, K. M., Ed.; The Electrochemical Society, Pennington, NJ, 1995; Vol. VII, p 654.
(15) (a) *Ultrasound: Its Chemical, Physical and Biological Effects*; Suslick, K. S., Ed.; VCH: Weinheim, 1988. (b) Suslick, K. S.; Choe, S. B.; Cichowlas, A. A.; Grinstaff, M. W. *Nature* **1991**, *353*, 414. (c) Koltypin, Yu.; Katabi, G.; Prozorov, R.; Gedanken, A. *J. Noncryst. Solids* **1996**, *201*, 159. (d) Hyeon, T.; Fang, M.; Suslick, K. S. *J. Am. Chem. Soc.* **1996**, *118*, 5492. (e) Cao, X.; Koltypin, Yu.; Katabi, G.; Felner, I.; Gedanken, A. *J. Mater. Res.* **1997**, *12*, 405. (f) Arul Dhas, N.; Gedanken, A. *J. Phys. Chem. B* **1997**, *101*, 9495.
(16) Stobers, W.; Fink, A.; Bohn, E. *J. Colloid Interface Sci.* **1968**, *26*, 62.

denum hexacarbonyl (1 g) and activated silica (300 mg) in 100 mL of decane was exposed to a high-intensity ultrasonic horn (direct immersion) at room temperature for 3 h, under ambient air. The temperature of the reaction mixture (slurry) rose to 90 °C during sonication, as measured using an IC thermocouple. On irradiation, the colorless slurry turned blue, which gradually became more intense with increased irradiation. The appearance of the blue color is due to the generation of pentavalent molybdenum oxide. The observed gradually increased intensity of the color indicates the formation of a blue product as irradiation time progressed. The reaction was carried out for 3 h to complete the decomposition of the molybdenum carbonyl in the reaction mixture; otherwise the MOS would have been contaminated by the $Mo(CO)_6$. The resulting powder was recovered by centrifugation, washed several times with dry pentane, and dried in a vacuum. The sonochemical decomposition of the coating precursor to the coating phase ($Mo_2O_5 \cdot xH_2O$) was confirmed by the FT-IR spectroscopy (see later). The characterization of $Mo_2O_5 \cdot xH_2O$ was described in our earlier paper.[15f]

Sonochemical Synthesis of MCS. All manipulations to prepare MCS composite were carried out in an inert atmosphere condition. To obtain MCS composite, 300 mg of activated silica and 1 g of $Mo(CO)_6$ in 100 mL of decane were sonicated under a dry argon atmosphere for 3 h. The solutions to be sonicated were purged with dry argon gas and were kept under an argon atmosphere throughout the experiment. The sonication was carried out under similar conditions, as described above. The resulting black powder was recovered by centrifugation, washed several times with dry pentane, dried in a vacuum, and preserved in vials in an inert atmosphere glovebox (O_2 level <10 ppm). The characterization of bulk molybdenum carbide generated by sonication has been described elsewhere.[15d]

Characterization. The phase composition and nature of the product powders was determined by XRD, using a Rigaku 2028, Cu Kα diffractometer. The overall morphologies of the coated and uncoated silica particles were obtained by TEM, using a JEOL-JEM 100SX electron microscope. Samples for the TEM measurements were obtained by placing a drop of suspension from the as-sonicated reaction mixture on a carbon-coated Formvar copper grid (400 mesh, Electron Microscopy Sciences), followed by air-drying to remove the solvent. The UV−visible spectra of the MOS was obtained using a Varian (model DMS 100S) UV−visible spectrophotometer. IR spectra were recorded using a Nicolet (impact 410) FT-IR spectrometer, using transparent pellets of the compounds in KBr (Aldrich, FT-IR grade) matrixes. KBr was used as the background file. All spectra were measured from approximately 4000 to 400 cm^{-1}, and the number of scans was typically 75, with a resolution of 4 cm^{-1}.

Results and Discussion

Powder X-ray analysis. Amorphous activated silica prepared by Stober's method followed by calcination was used in this study. The powder X-ray diffraction of as-made MOS and MCS showed the absence of diffraction peaks (Figure 1a,b). The absence of an XRD peak indicated that either the particles were crystallographically amorphous in nature or that the crystalline domains were too small to give rise to a crystal reflection in the XRD pattern. However, the amorphous nature of these powders was further confirmed by the selectd area electron diffraction (SAED) pattern, using TEM (see below), and these powders demonstrated a diffuse ring pattern characteristic of amorphous materials. The XRD pattern of the MCS composite after calcining it at 450 °C under the flow of N_2 for 2 days showed the presence of diffused peaks, corresponding to the Mo_2C phase (Figure 1c). The broad nature of the XRD peaks could be due to the presence of partially ordered or weakly crystalline Mo_2C nanoparticles. The diffraction

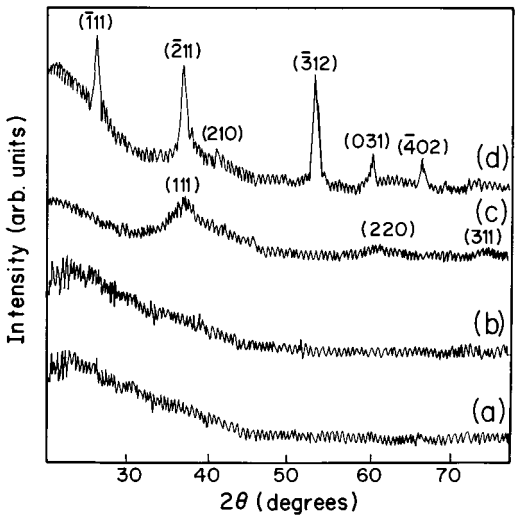

Figure 1. Powder XRD patterns of (a) as-made MOS, (b) as-made MCS, (c) calcined MCS, and (d) calcined MOS.

patterns are indexed on the basis of JCPDS data. At this level, the relatively weak crystalline nature of the Mo_2C in MCS could be attributed to the interplay of the chemical interaction between Mo_2C and SiO_2 and the inert thermal nature of Mo_2C, which influences the crystallization process.

Heating the MOS at 450 °C for 2 days in a flow of H_2 yielded a black powder, and diffraction peaks were observed that corresponded to the MoO_2 phase exclusively (Figure 1d). All possible MoO_2 peaks were present, indicating the polycrystallinity of the MoO_2 phase. The broad nature of the XRD peak dictated the ultrafine nature of the crystalline coating phase. It is surprising to note that under these thermal conditions MOS did not yield any XRD peak corresponding to metallic Mo. On the other hand, reduction of bulk Mo_2O_5 under the same thermal conditions yielded a mixture of metallic Mo and MoO_2 phases.

A good correspondence between the thermal characteristics and the chemical interaction was expected because the reducibility of molybdenum oxide in MOS depends on the interaction strength. Several researchers have inferred a "weak-type" interaction, accounting for an easy reduction of the MoO_3-SiO_2 catalyst.[8a,17] In the literature, the evidence for the occurrence of a stepwise reduction of $Mo^{VI} \rightarrow Mo^{IV} \rightarrow Mo^{o}$ in the temperature range of 400−900 °C of supported MoO_3 has been reported. We have carried out the phase evolution of MOS by long-term thermal reduction at a relatively low temperature (450 °C for 1−7 days), as the sonochemical process usually yields highly reactive nanoparticles.[15] X-ray diffraction patterns of products obtained by the thermal reduction of MOS are presented in Figure 2. Heating the MOS at 450 °C for 2 days in a flow of H_2 yielded the pure MoO_2 phase. However, a further increase in the heating period, without any intermittent grinding, yielded a mixture of metallic Mo and MoO_2 phases (Figure 2b). Heating the MOS for 4 days yielded metallic Mo as a major phase, with a minor MoO_2 phase. The (110), (200), and (211) XRD reflections of metallic Mo can be clearly seen (Figure 2c). The increase in the intensity of metallic Mo XRD peaks may

(17) Arnoldy, P.; de Jonge, J. C. M.; Moulijin, J. A. *J. Phys. Chem.* **1985**, *89*, 4517. Regalbuto, J. R.; Ha, J. W. *Catal. Lett.* **1994**, *29*, 189.

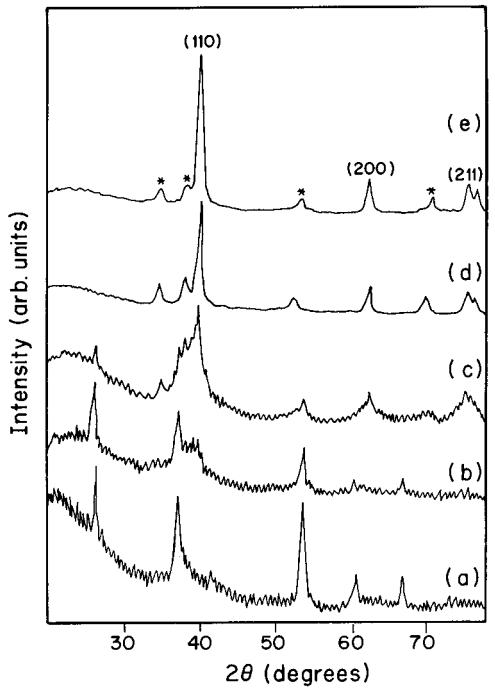

Figure 2. XRD patterns of MOS reduced at 450 °C for different periods: (a) 2 days, (b) 3 days, (c) 4 days, (d) 5 days, and (e) 7 days (* denotes MoO_2 phase).

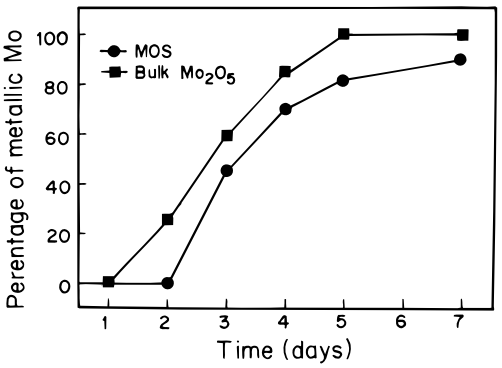

Figure 3. Percentage of metallic Mo against the reduction time.

be due to the reduction of MoO_2 phase upon heat treatments for a longer period. On further increase in the reduction time, the intensity of the XRD peaks corresponding to the metallic phase gradually increased, while the MoO_2 peaks decreased. Even heating the MOS for 5−7 days, with intermittent grinding, yielded, again, the MoO_2 impurity phase, as evidenced by the XRD reflections (Figure 2d,e). No characteristic peak due to the compound formation (Mo−Si−O ternary phases) between Mo_2O_5 and SiO_2 phases were observed.

From the intensity data of the XRD peaks, the fraction of the metallic Mo ($f_{(Mo)}$) was calculated using the following formula:

$$f_{(Mo)} = I(110)_{Mo}/[I(110)_{Mo} + I(\bar{3}12)_{MoO_2}] \qquad (1)$$

where $I(110)_{Mo}$ is the intensity of (110) molybdenum reflection and $I(\bar{3}12)_{MoO_2}$ is the intensity of the $(\bar{3}12)$ MoO_2 reflection. The percentage of metallic molybdenum formed in MOS and bulk Mo_2O_5 as a function of reduction time is plotted in Figure 3. From the plot it is evident that the MoO_2 phase transforms into Mo gradually, as the heating period is progressively increased. After heating the product at 450 °C for 4 days, about 70% of the MoO_2 is converted to metallic Mo in MOS, while 85% Mo is formed in bulk Mo_2O_5 under the same conditions. However, MoO_2 in MOS converted at a maximum of 85−90% of metallic Mo, after reduction for 6−7 days, while the bulk Mo_2O_5 was completely converted into metallic Mo. An interesting point to mention here is that a large difference in the reducibility is always maintained between the bulk Mo_2O_5 and the MOS. This lower reducibility of Mo_2O_5 in MOS, compared to bulk Mo_2O_5, demonstrates that a "strong-type" interaction occurred in the MOS composite.

Therefore, the thermal evolution of phases of MOS indicates that the amorphous Mo_2O_5 does not undergo a single step reduction to metallic Mo, rather, it initially yields MoO_2 and then metallic Mo clusters, consistent with the following reactions:

$$Mo_2O_5 + H_2 \rightarrow 2MoO_2 + H_2O \qquad (2a)$$

$$2MoO_2 + 4H_2 \rightarrow 2Mo + 4H_2O \qquad (2b)$$

$$Mo_2O_5 + 5H_2 \rightarrow 2Mo + 5H_2O \qquad (2)$$

Powder XRD results imply that the tightly bound nature of Mo_2O_5 results in a strong chemical interaction with the silica carrier, which in turn influences the reducibility of Mo_2O_5 to metallic Mo.

TEM Studies. The nature and morphology of the uncoated silica and sonochemically coated silica powders was examined using TEM. The morphology of the uncoated silica, sonochemically generated bulk Mo_2O_5, and Mo_2C powders is shown in Figure 4. TEM images of silica (Figure 4a) show the clean and smooth surface, without any foreign impurities. The uncoated silica particles were spherical in shape, monodispersed, and free of agglomeration. The mean diameter in the TEM micrograph was roughly around 250 nm. The TEM micrograph of Mo_2O_5 (Figure 4b) and Mo_2C (Figure 4c) shows the presence of porous and spongy nanoparticles, present in the form of small clusters. The average size of these porous nanoparticles are in the range of 5−10 nm and are held together in an irregular assembly of aggregate network. The extent of aggregate network formation in the Mo_2C clusters is larger than in the Mo_2O_5 clusters. The insets are the corresponding SAED patterns, which show only a diffuse ring pattern characteristic of amorphous materials.

TEM micrographs of the MOS (Figure 5a,b) and the MCS (Figure 5c,d) reveal the nature of the carrier and coating particulates. Both MOS and MCS powder consists of silica spheres coated with clusters of Mo_2O_5 and Mo_2C, respectively. The silica core, as well as the coating clusters, has almost the same morphology, even after the sonochemical coating. It can be seen that the Mo_2O_5 clusters generated by the sonochemical decomposition of $Mo(CO)_6$ are strongly attached to the surface of silica (Figure 5a,b). The sonochemically generated porous nanoparticles are found as clusters, but the carrier silica particles are not. Each silica sphere is completely coated by the Mo_2O_5 clusters, without any free silica surface. The central silica core is coated with a regular periphery of Mo_2O_5 clusters. The coating thickness is fairly uniform throughout the silica surface and is around 10−20 nm. On the other hand, the MCS composite shows (Figure 5c,d) a nonuniform coating of

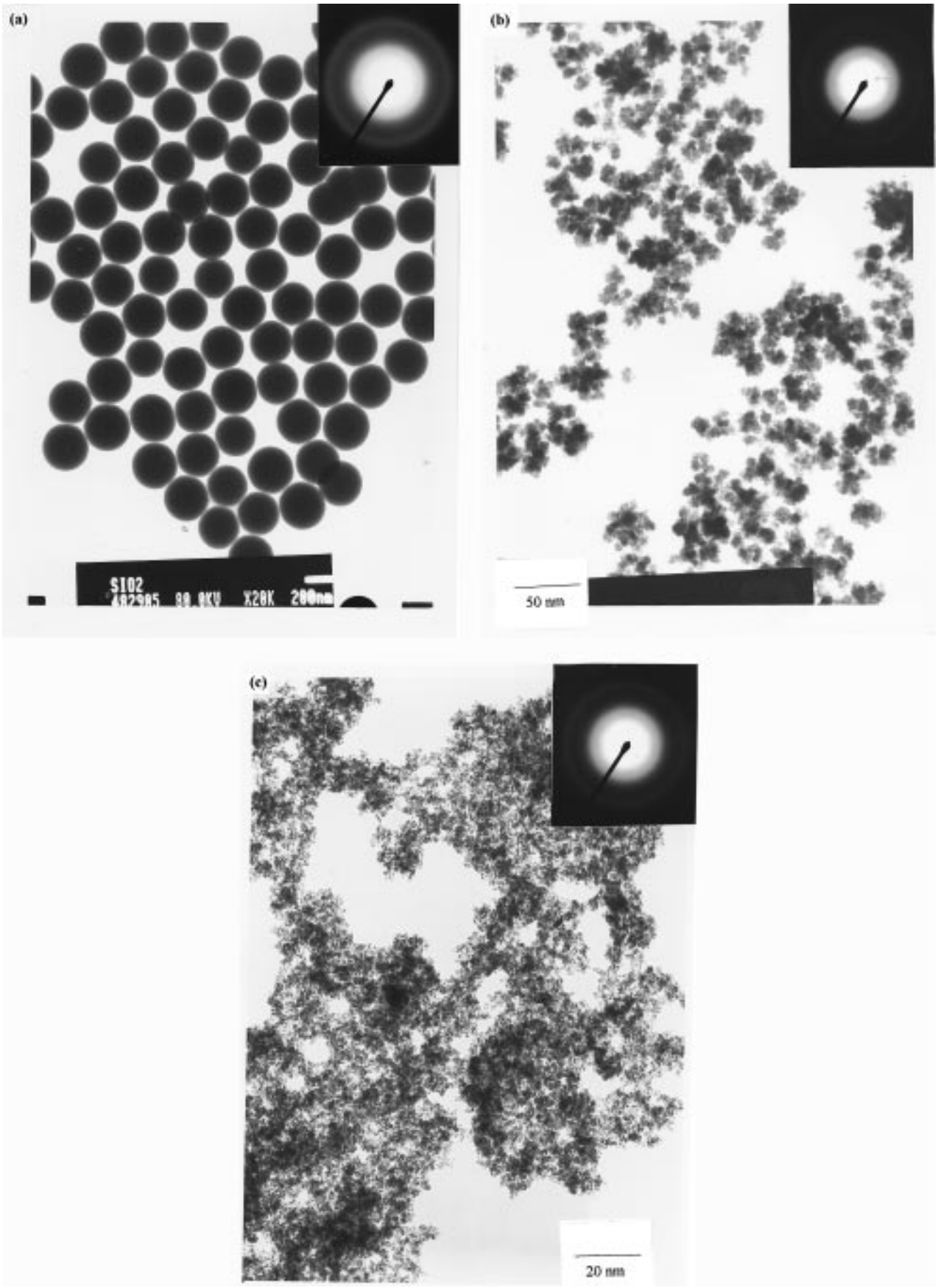

Figure 4. TEM micrograph: (a) uncoated silica, (b) Mo_2O_5, and (c) Mo_2C (inset, associated SAED pattern).

the Mo_2C on silica, resulting in heaps and free particles. The spongy Mo_2C particles are irregularly attached on the silica as nanoparticles. The heaps of Mo_2C are piled up over the surface, resulting in a large number of Mo_2C aggregates. A relatively large bare surface of silica remains uncoated. Even at the lowest Mo mass loading used in this study (sample C4), almost identical behavior was observed. The morphology of the calcined MCS

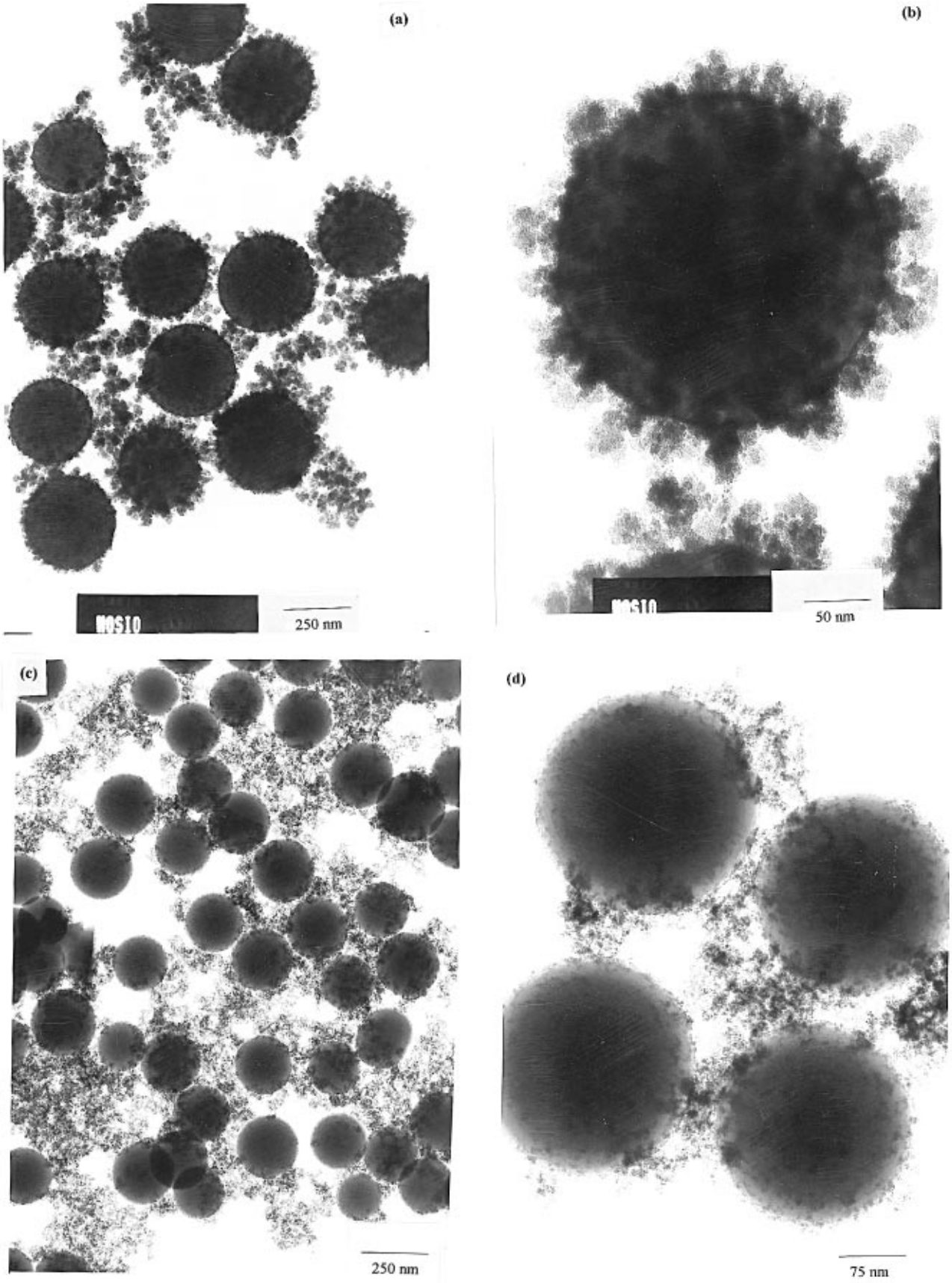

Figure 5. TEM micrograph: (a and b) MOS at two different magnifications and (c and d) MCS at two different magnifications.

nanocomposite again showed poor attachment of the Mo_2C. The Mo_2C clusters lost their porous nature and were transformed into more dense aggregates upon calcination. The nonuniform coatings and poor adhesion of Mo_2C, compared to that of the Mo_2O_5 on silica, is perhaps due to its inert chemical nature, which was translated into less efficient scavenging. This led to a collection of separate Mo_2C and uncoated silica particles.

We have examined the TEM microstructure of MOS nanocomposite with different Mo_2O_5 loadings, since it

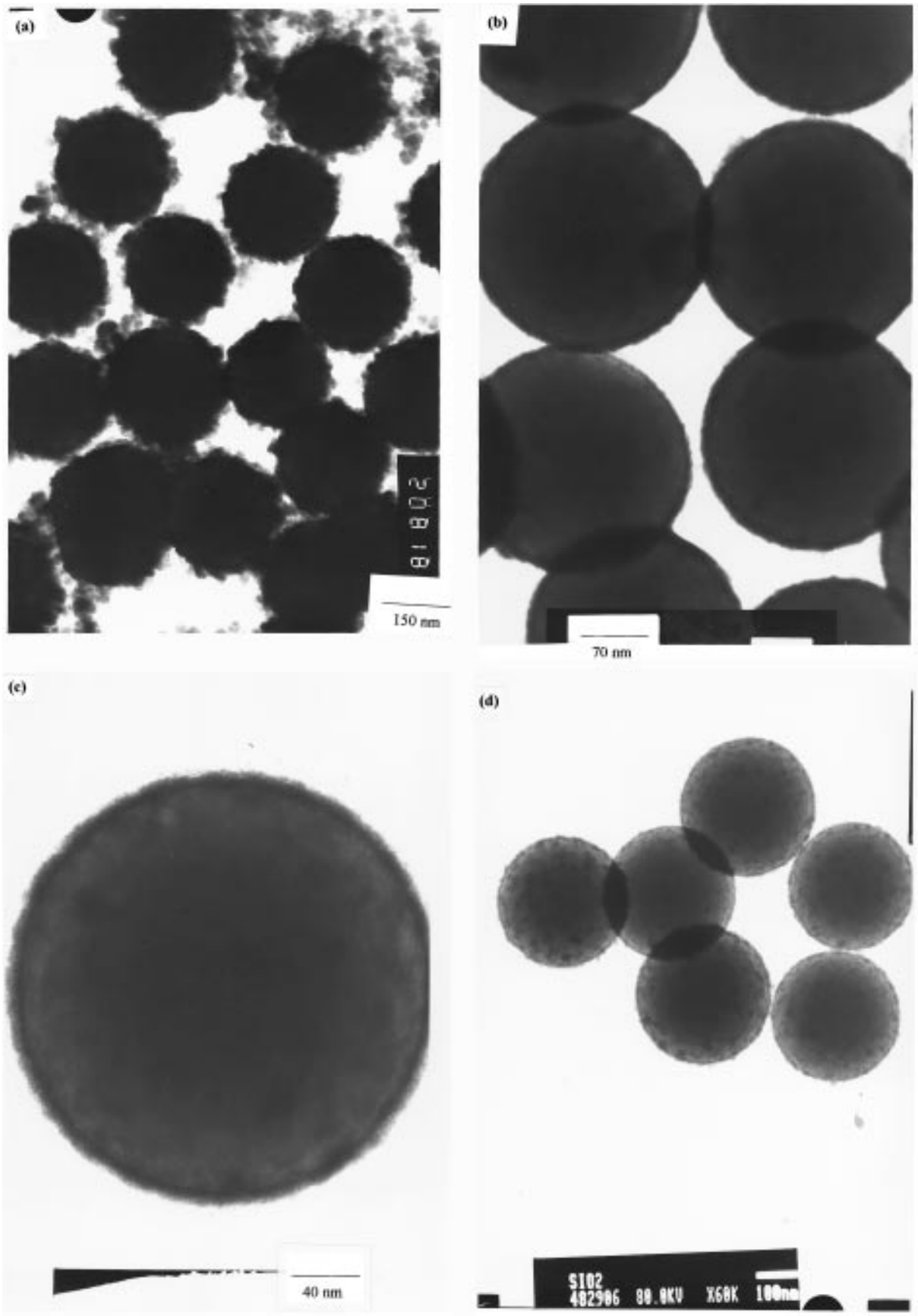

Figure 6. TEM image of MOS at different Mo concentrations: (a) C2 sample, (b and c) C3 sample (two different magnifications), and (d) C4 sample.

shows interesting coating characteristics compared to those of MCS materials. Representative TEM micrographs of MOS with different loadings, namely, samples C2, C3, and C4, are depicted in Figure 6. It is gratifying to observe that uniform and dense coatings are obtained at low Mo_2O_5 mass loading (C2) (Figure 6a). Under these conditions, almost all the silica spheres are completely coated by the clusters of the Mo_2O_5 nano-

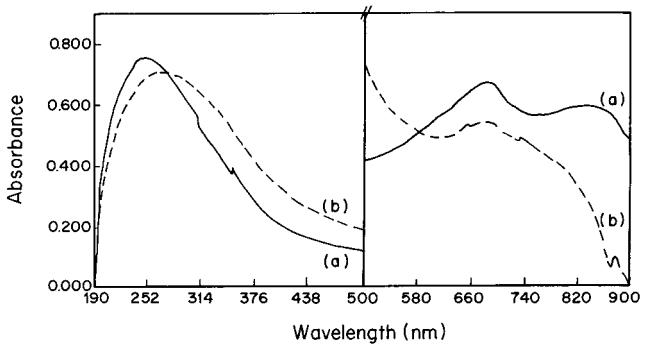

Figure 7. UV−visible spectra: (a) Mo_2O_5 and (b) MOS.

particles, without any bare silica zones. A negligible amount of collection of free Mo_2O_5 is observed. As the Mo concentration decreases (C3), the silica spheres are coated with a thin layer of Mo_2O_5, rather than clusters (Figure 6b). Under these conditions, no free Mo_2O_5 was observed and all the formed Mo_2O_5 nanoparticles are coated on the silica carrier. A magnified TEM image of MOS with C3 concentration (Figure 6c) reveals uniform coating of the Mo_2O_5 nanoparticles as a thin layer of less than 10 nm. The central silica core is coated with a regular periphery of a thin layer of nanoparticles of Mo_2O_5. At the lowest level of initial Mo concentration (C4), almost all the silica spheres are completely coated by nanoparticles of Mo_2O_5 (Figure 6d).

UV−Visible Studies. To obtain information about the nature and the local structure around the metal ion in the amorphous MOS composite, UV−visible spectroscopy was applied. The UV−visible spectra (Figure 7) of the bulk Mo_2O_5 and MOS in acetonitrile shows absorption in both UV and visible regions. Bulk Mo_2O_5 shows two absorption bands in the visible region at around 820 and 670 nm, characteristics of Mo^V, a d^1 system. The electronic spectra of the simple Mo^V oxide can, in principle, display d−d transitions, in which the single unpaired electron is promoted from the d_{xy} orbital to the doubly degenerate Mo=O (π^*) level or to the two higher d(σ^*) levels.[18] In comparison with the spectra of Mo^V compounds,[18b] the maxima observed at 820 nm band led to the assignment of a $^2B_2 \rightarrow {}^2B_1$ transition (intervalence band), with the other visible band at 670 nm corresponding to a $^2B_2 \rightarrow {}^2E$ transition. The absorption band of MOS composite at 670 nm in the visible region is essentially the same as the bulk Mo_2O_5. On the other hand, the intervalence absorption band at around 820 nm of the bulk Mo_2O_5 disappeared and became a diffused hump when coated on silica (Figure 7b). The disappearance of the intervalence transition band very likely stems from the formation of interfacial bond Mo−O−Si, limiting the extent of the intervalence transition of the Mo in MOS.

The broad absorption band (200−350 nm) centered at around 250 nm in the UV region is ascribed to the expected ligand−metal charge transfer (LMCT) bands originating from the promotion of electrons from the filled Mo=O (π) levels to the d orbitals. The position of the LMCT absorption band is known to be sensitive to the local symmetry of metal ion.[19a] For oxygen ligands,

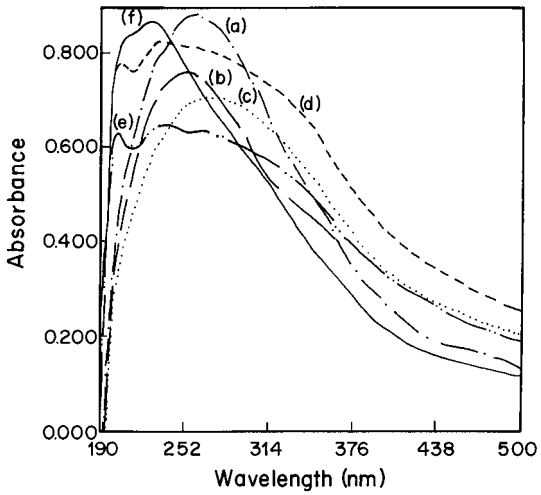

Figure 8. LMCT absorption spectra of MOS at different Mo concentrations: (a) bulk Mo_2O_5, (b) C1 sample, (c) C2 sample, (d) C3 sample, (e) C4 sample, and (f) uncoated silica.

a more energetic transition is expected for a tetrahedral-coordinated Mo than for an octahedral one. The [MoO_4] and [MoO_6] LMCT bands normally appear at the 220−270 nm and 270−340 nm ranges, respectively. Distortion of the symmetry of the [MoO_6] or [MoO_4] structure would cause the LMCT band to shift to a shorter wavelength. The observed broad nature of the LMCT absorption band of the bulk Mo_2O_5 cannot be ascribed to a simple type of geometry (T_d or O_h); however, it can be attributed to the existence of both [MoO_4] tetrahedra (T_d) and [MoO_6] octahedra (O_h) having a distorted symmetry. Pronounced change in the peak position, as well as peak shape, was observed for the MOS LMCT band (Figure 7b). A shift of 10−15 nm to a longer wavelength and more broadening of the LMCT band were detected for MOS. The change in the absorption profile of MOS was probably due to the formation of an interfacial bond, as expected.

To understand the surface bonding nature of SiO_2 and Mo_2O_5 in MOS, we have studied the LMCT band of MOS with different Mo loading (Figure 8). For the purpose of comparison, the LMCT bands of bare silica and bulk Mo_2O_5 are also included in Figure 8. At a higher Mo loading (concentration), the absorption bands are similar to that of the bulk Mo_2O_5 (Figure 8a−c). Pure silica shows (Figure 9f) a broad peak centered at 220 nm, with a shoulder at around 205 nm, corresponding to O → Si charge transfer.[19b] Upon Mo_2O_5 coating, the LMCT band corresponding to the silica splits into two distinct peaks (Figure 8e,d). Two absorption bands near 220 and 205 nm appeared for the MOS at C4 composition (see Table 1). The long tail of up to 350 nm of the LMCT band is due to absorption of the Mo ions. The observed split in the LMCT band of silica at a low concentration of Mo_2O_5 probably arises from the formation of an interfacial band Si−O−Mo, to some extent thereby influencing the LMCT absorption. On further increase in the Mo concentration, the splitting of the LMCT band of SiO_2 becomes less prominent and behaves like that of a composite of silica and Mo_2O_5 (Figure 8b,c).

Infrared Studies. Infrared (IR) spectra of the reactant and the product (MOS and MCS) (Figure 9)

(18) (a) Ung, V. A.; Bardwell, D. A.; Fjeffery, J. C.; Maher, J. P.; McCleverty, J. A.; Ward, M. D.; Williamson, A. *Inorg. Chem.* **1996**, *35*, 5290. (b) Manoharan, P. T.; Rogers, M. T. *J. Chem. Phys.* **1968**, *49*, 5510.

(19) (a) Aritani, H.; Tanaka, T.; Funabiki, T.; Yoshida, S.; Eda, K.; Sotani, N.; Kudo, M.; Hasegawa, S. *J. Phys. Chem.* **1996**, *100*, 19495. (b) Shi, Y.; Seliskar, C. J. *Chem. Mater.* **1997**, *9*, 821.

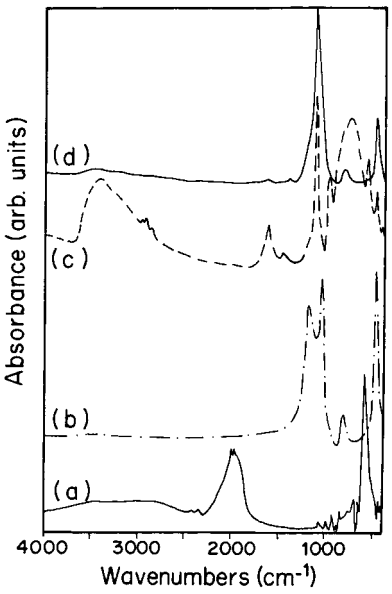

Figure 9. FT-IR spectra: (a) $Mo(CO)_6$, (b) uncoated silica, (c) MOS, (d) MCS.

lend support to our observation of the sonochemical decomposition of $Mo(CO)_6$ to molybdenum oxide and molybdenum carbide under air and argon atmospheres, respectively. A band at 2000 cm^{-1} in the spectrum of $Mo(CO)_6$ (Figure 9a), which is diagnostic[20] of the carbonyl stretching vibration, disappears in the products, MOS (Figure 9c) and MCS (Figure 9d). Also, the product MOS shows (Figure 9c) IR absorption bands in the region of 600−1000 cm^{-1}, corresponding to the Mo═O and Mo−O vibrational modes. A sharp absorption band of around 960 cm^{-1} is characteristic of terminal molybdenum oxygen double bond (Mo═O) stretching, indicating the presence of a strong molybdenum−oxygen bond of the molybdenyl type. The strong diffuse absorption band between 900 and 600 cm^{-1} corresponds to the overlapping of vibrational bands of Mo−O single bonds and Mo−O−Mo linkages in an octahedral, as well as tetrahedral, symmetry.[21] The Mo ions in the "blue oxides" can exhibit two types of coordination—tetrahedral coordination and more common octahedral coordination—and thus they may have T_d or O_h symmetry with respect to oxygen atoms. In general, the IR spectra of Mo blue oxides are quite complex, owing to the two types of symmetry groups, of T_d and O_h.[21b] The presence of water molecules in the initial product yields a broad absorption between 3000 and 3600 cm^{-1} and 1600 cm^{-1}, corresponding to the OH stretching and bending modes, respectively. On the other hand, the MCS primarily shows (Figure 9d) the absorption bands that correspond to the silica in the IR region.

The IR spectrum of the activated silica shows (Figure 9b) three absorption bands in the region of 1600−400 cm^{-1}, characteristic of the siloxane links.[22] The absorption band at ∼460 cm^{-1} correspond to the racking mode, while the band at ∼810 cm^{-1} is due to the symmetric stretching of the Si−O−Si group.[22] The observed broad doublet band in the wavenumber region of 1200−1000 cm^{-1} corresponds to the asymmetric stretching (AS) vibrational mode of the Si−O−Si bridge of the siloxane link. The sharp band at 1060 cm^{-1} corresponds to the characteristic oxygen asymmetric stretch mode (AS). The splitting of the AS mode of the activated silica is probably due to the presence of strained siloxane links (disorder-induced coupling), as recognized earlier.[23,24]

The IR spectrum of MOS (Figure 9d) and MCS (Figure 9e) shows a significant change in the absorption profile of the silica component. A pronounced change was noticed in the IR spectral region of the AS mode of the siloxane link. The doublet of the activated silica AS band was replaced by a sharp band near 1110 cm^{-1}, corresponding to the AS mode and indicating a surface modification of the Mo species coating by ultrasonic cavitation. A higher frequency shift of 50 cm^{-1} was observed for the AS mode upon coating, probably associated with the bonding change around the $[SiO_4]$ tetrahedra. The splitting of the AS mode of SiO_2 disappeared upon sonochemical deposition of the Mo species on the SiO_2 surface. However, a less intense small shoulder in the region of 1200 cm^{-1} could still be detected, typifying a low degree of disorder splitting due to the depletion of strained siloxane networks of amorphous SiO_2 upon sonochemical coating. Thus, the decreased intensity of the splitting of AS mode reveals surface ordering by breaking the strained siloxane networks of the silica upon ultrasound cavitation. The marked change in the nature, as well as peak position, of the AS mode of the silica in MOS and MCS could be related to ultrasound-induced surface modification of silica (breaking of strained Si−O−Si links), which facilitates the Si−O−Mo interfacial bond. The breakage of the strained siloxane link by ultrasonic cavitation seems to be energetically preferable because it allows reduction of the structural tensions in this fragment (Si−O−Si), owing to the greater length and lower rigidity of the free Si−O bond.[25]

Bonding in MOS and MCS Nanocomposites. The interaction between the oxide species, carbides, or metals and the silica surface is explained by the bonding contributions via chemical interaction between the support and active phase (formation of interfacial bonds).[26−31] Zingg et al.[26] have identified the presence of both tetrahedrally and octahedrally coordinated Mo species in $Mo-Al_2O_3$ catalyst. They claim that the presence of tetrahedrally coordinated Mo^{VI} oxide species reduced to tetrahedrally coordinated Mo^{V} oxide species under thermal reduction is responsible for the good adhesion and distribution of the active phase on the support material. Several research groups have studied the interaction between the silica carrier and surface

(20) Nakamoto, K. *Infrared Spectra of Inorganic and Coordination Compounds*, Wiley: New York, 1963.
(21) (a) Li, C.; Xin, Q.; Wang, K.-L.; Guo, X. *Appl. Spectrosc.* **1991**, *45*, 874. (b) Anvar, M.; Hogarth, C. A.; Theocharis, C. R. *J. Mater. Sci.* **1989**, *24*, 2387.
(22) Kirk, C. T. *Phy. Rev. B* **1988**, *38*, 1255. Hu, S. M. *J. Appl. Phys.* **1980**, *51*, 5945.
(23) Almeida, R. M.; Pantano, C. G. *J. Appl. Phys.* **1990**, *68*, 4225.
(24) Gaskell, P. H.; Johnson, D. W. *J. Non-Cryst. Solids* **1976**, *20*, 153. Gaskell, P. H.; Johnson, D. W. *J. Non-Cryst. Solids* **1976**, *20*, 171.
(25) Pelmenschikov, A. G.; Morosi, G.; Gamba, A. *J. Phys. Chem.* **1991**, *95*, 10037.
(26) Zingg, D. S.; Makovsky, L. E.; Tischer, R. E.; Brown, F. R.; Hercules, D. M. *J. Phys. Chem.* **1980**, *84*, 2898.
(27) Williams, C. C.; Ekerdt, J. G.; Jehng, J.-M.; Hardcastle, F. D.; Turek, A. M.; Wachs, I. E. *J. Phys. Chem.* **1995**, *95*, 8781.
(28) Gambaro, L. A.; Fierro, J. L. G. *React. Kinet. Catal. Lett.* **1981**, *18*, 495.
(29) Che, M.; Louis, C.; Tatibouet, J. M. *Polyhedran*, **1986**, *5*, 123.
(30) Hucul, D. A.; Brenner, A. *J. Phys. Chem.* **1981**, *85*, 496.
(31) Asakura, K.; Iwasawa, Y. *Chem. Lett.* **1986**, 859.

Mo species.[27] The nature of bonded sites on supported molybdena catalysts has been the subject of controversy in the literature. The bonding of the molybdate species to the silica surface is likely to be covalent in nature. The molybdate species is usually represented as the negatively charged species, $(MoO_4)^{2-}$. Similarly, because of the high acidity of silica, the polarity of Si−O bonds in silica is $Si-O^-$. Because the direction of polarization in both species is the same, bonding results in a complex that is neutral in character, with relatively weak covalent Si−O−Mo bonds.[27] Gamboro and Fierro[28] indicated that on MoO_3-SiO_2 adsorption occurs on Mo^{5+} (pentavalent) sites. Che et al.[29] have prepared a dark brown Mo_2Cl_{10} on SiO_2 by reacting $MoCl_5$ with silica hydroxyl groups. Upon exposure to air, this became dark blue, indicative of the hydrolysis and partial oxidation of Mo_2Cl_{10} to the Mo^V oxide, which is chemically bound to the silica surface. From the EPR and UV−visible studies of $Mo-SiO_2$ systems, the formation of a strong chemical bond (Si−O−Mo) seemed to result from a high degree of covalency of the molybdenyl Mo^V oxide species in a tetrahedral symmetry. Che et al.[29] were able to identify three types of coordination spheres of Mo^{5+} ions. Under similar bonding interactions, the formation of a Si−O−Mo interfacial link leading to a strong surface attachment of the Mo_2O_5 to the silica surface can be reasonably assumed. The formation of strong interfacial chemical bonds in MOS under cavitation could be favored by the following two factors: (i) the $Si-O^-$ nucleating sites formed by the ultrasonic breakage of strained siloxane links can expected to be more facile in the formation of interfacial bonds; and (ii) the high degree of the covalent character of the $(Mo{=}O)^{3+}$ in the Mo_2O_5 leads to a strong interfacial chemical bond.

The study of the nature of the interaction between the ceramic metal carbides and the ceramic oxide support is limited.[12] It is generally accepted that the "weak-type" interaction occurring between Mo_2C and the SiO_2 support accounts for a poor dispersion or coating. This is a consequence of the inert nature of Mo_2C. However, the $Si-O^-$ sites generated by the breakage of strained Si−O−Si links upon cavitation could serve as nucleating centers for the formation of moderately strong interfacial bonds with the Mo_2C phase.

The above results demonstrate that the ultrasound-induced cavitation appears to play a dual role in the decomposition of molybdenum carbonyl, as well as in the activation of the silica surface for the adhesion of the resulting Mo species.

Sonochemical Reaction Mechanism. Most of the chemical reactions, which are brought about by ultrasonic waves intense enough to produce cavitation, are oxidation and decomposition.[32−35] The sonochemical reaction can be understood by considering the reaction sites: (i) the gas phase within the collapsing cavity "bubble", where elevated temperatures and high pressures are produced, and (ii) the interfacial region or liquid phase immediately surrounding the gas-phase region, where the temperature is lower than in the gas-phase reaction zone but still high enough for a sonochemical reaction.[15a] The sonochemical implosive collapse of the bubble generates high-speed shock waves, which help to disperse the reaction mixture uniformly. The sonochemical decomposition of molybdenum hexacarbonyl would not occur in the bubble, due to its low vapor pressure, even at 90 °C. Therefore, the sonochemical reaction of $Mo(CO)_6$ appears to take place in the interfacial region. The decomposition temperature of $Mo(CO)_6$ is approximately 150 °C, implying that high-temperature sonochemical decomposition of $Mo(CO)_6$ is necessary to drive the decomposition to completion, compared to that of the sonochemical decomposition of other volatile transition metal carbonyls, such as $Fe(CO)_6$ and $Ni(CO)_4$. The sonochemical decomposition of $Mo(CO)_6$ in the presence of atmospheric air or O_2 and the formation of MOS may be written as:

$$2Mo(CO)_6 + {}^{17}/_{2}O_2 \rightarrow Mo_2O_5(s) + 12CO_2(g) \quad (3a)$$

$$Mo_2O_5 + SiO_2 \rightarrow Mo_2O_5{-}SiO_2 \quad (3b)$$

$$2Mo(CO)_6 + SiO_2 + {}^{17}/_{2}O_2 \rightarrow Mo_2O_5{-}SiO_2(s) + 12\,CO_2(g) \quad (3)$$

On the other hand, the sonochemical formation of MCS composite from $Mo(CO)_6$ and SiO_2 under an argon atmosphere can be written as

$$2Mo(CO)_6 \rightarrow 2Mo(s) + 12CO(g) \quad (4a)$$

$$2CO \rightarrow C(s) + CO_2(g) \quad (4b)$$

$$2Mo + C \rightarrow Mo_2C(s) \quad (4c)$$

$$Mo_2C + SiO_2 \rightarrow Mo_2C{-}SiO_2(s) \quad (4d)$$

$$2Mo(CO)_6 + SiO_2 \rightarrow Mo_2C{-}SiO_2(s) + CO_2(g) + 10\,CO(g) \quad (4)$$

The in situ generated Mo (eq 4a) and atomic C (eq 4b) react under sonochemical conditions to generate Mo_2C (eq 4c). The formation of clusters of the coating phase may be due to the collision of freshly formed monomers of Mo_2O_5 (eq 3a) or Mo_2C (eq 4c). The coating clusters then collide with the silica carrier under the influence of shock waves produced by the implosive bubble collapse (microstreaming effect) and are deposited on the silica surface. The microstreaming effect is known to accelerate the mass transport processes, leading to the morphological change or activation of the particulate surfaces.[35] At a low precursor concentration, the collision between the formed coating phase is less probable, thereby causing them to deposit as thin layers or as nanoparticles on the silica carrier.

Conclusion

The surface coating of silica microspheres by molybdenum oxide and molybdenum carbide clusters has been successfully accomplished by the sonochemical decomposition of $Mo(CO)_6$ followed by in situ deposition under

(32) Suslick, K. S.; Gawlenowski, J. J.; Schubert, P. F.; Wang, H. H. *J. Phys. Chem.* **1983**, *87*, 2299.
(33) Margulis, M. A. *Advances in Sonochemistry* Vol. 1, Mason, T. J., Ed.; JAI press: London, 1990; p 39.
(34) Guierrez, M.; Henglein, A.; Dohrmann, J. K. *J. Phys. Chem.* **1987**, *91*, 6687.
(35) Pugin, B.; Turner, A. T. *Advances in Sonochemistry*; Mason, T. J., Ed.; JAI press: London, 1990; Vol. 1, p 81.

air and argon atmospheres, respectively. The precursor molybdenum hexacarbonyl serves as an in situ source for both of the species. Powder X-ray diffraction patterns show the amorphous nature of the composite product, which on further calcination yields stable crystalline phases. Evidence of a strong molybdenum oxide−silica carrier interaction depressing the thermal reducibility of the MOS has been demonstrated. The TEM studies on MOS composite revealed strong adhesion, a well-dispersed nature, and a uniform coating of the molybdenum oxide on the silica surface. Low concentrations of $Mo(CO)_6$ allowed molybdenum oxide to spread a uniform coating as thin layers or as nanoparticles on silica carrier, without any collection of the free coating phase. The TEM image of MCS composite showed irregular coating, and heaps of Mo_2C piled out from the silica surface, indicating a "weak-type" interaction. The formation of a strong interfacial bond, Si−O−Mo in the MOS, is demonstrated in the change in the absorption profile of the intervalence band of Mo_2O_5, as well as in the LMCT band of silica. FT-IR absorption spectroscopy studies on MOS and MCS composite demonstrate that the amorphous silicon dioxide undergoes structural reorganization (breakage of strained siloxane links), followed by the formation of Si−O−Mo interfacial linkage upon sonochemical deposition of the coating phase. The relatively strong chemical interaction in MOS, compared to that of MCS nanocomposite, is likely to result from the presence of pentavalent $(Mo{=}O)^{3+}$ sites. The sonochemically prepared MOS and MCS composites appear to meet the "design criteria" and thus promise to have superior catalytic activity than do the conventional materials. The simultaneous use of ultrasound-induced cavitation to decompose the coating precursor and to activate the carrier surface may be applicable in the generation of a wide variety of technologically important coated materials.

Acknowledgment. We thank the Ministry of Science and Arts, Israel, for a Binational India-Israel grant. We thank Prof. Deutsch, Department of Physics, and Prof. Malik, Department of Life Sciences, for extending their facilities to us. The authors thank Dr. Shifra Hochberg for the help in preparing the manuscript.

CM9704488